AN EXPERIMENTAL INVESTIGATION OF A LITHIUM ALUMINUM HYDRIDE—HYDROGEN PEROXIDE HYBRID ROCKET

Ronald V. Osmon

The results of static test firings of a 230-lb. thrust hybrid rocket with lithium aluminum hydride used as the solid fuel and hydrogen peroxide as the liquid oxidizer are presented. The objective of the program was to determine the combustion and performance characteristics of the propellant combination experimentally.

A regression rate correlation was obtained which indicates that the regression of the solid fuel is moderately pressure sensitive. This is a desirable characteristic for applications requiring variable thrust. The test results show that the maximum specific impulse efficiency attained was about 80%, and the maximum C* efficiency was 86%. The expected increase in combustion efficiency through the use of turbulators did not occur, which is explained by apparent particle agglomeration at the grain surface.

The pressed fuel grains maintained their structural integrity at all times during the firings and had a smooth regression surface over the aft two-thirds of the grain length. Certain design aspects of a tubular fuel grain are discussed, based on the regression correlation obtained. For the tubular grain example given, it is practical to vary the thrust of a hybrid engine with these propellants by a factor of at least 11:1 with only about 2:1 reduction in oxidizer-to-fuel ratio.

One of the classic problems with many hybrid rockets is their inability to maintain a constant mixture ratio when the oxidizer flow is throttled down to reduce the thrust. Since the design mixture ratio O/F is that which yields the maximum specific impulse, any deviation in O/F must result in a lower delivered specific impulse, Isp. The primary reason for the O/F shift with throttling is that the convective heat transfer, which principally governs the regression rate for nonmetallized solid fuels, has a nonlinear dependence on the oxidizer flow rate. Several solutions to this problem have been suggested, all of which have some disadvantages. One solution is to find a hybrid propellant combination that has a nearly constant Isp for a wide range of mixture ratios; however, this presents a propellant utilization problem. Another solution is to inject part of the liquid oxidizer at the aft end of the fuel grain to bring the O/F back up to the design value. This solution would seem to nullify some of the advertised advantages of a hybrid such as simplicity and reliability. An ideal solution would be to find a hybrid propellant combination in which pressure has a dominant role in establishing the regression rate such that a reduction in chamber pressure produces a fuel flow proportional to the oxidizer flow. Propellants with high percentages of solid or liquid particles in their combustion products would be expected to have pressure-dependent regression rates, since radiation heat transfer between the particles and the grain surface (which is pressure dependent) would be significant. Such a propellant combination is lithium aluminum hydride and hydrogen peroxide, since its combustion products theoretically contain 63% by weight of aluminum oxide particles at the optimum mixture ratio.

Recent Norair calculations obtained with the computer program developed in reference *1* have established the peak Isp (1,000 ⟶ 14.7 lb./sq. in. abs., shifting equilibrium) of the lithium aluminum hydride–hydrogen peroxide propellant combination to be 301 sec. as shown in Figure 1. The corresponding bulk density is 1.13 g./cc. Certain operational advantages that stand out are the availability of both propellants, the wealth of experience and excellent logistics of 90% hydrogen peroxide, and the essentially nontoxic exhaust products. The storability and handling characteristics of 90% hydrogen peroxide are well known. Recently the storability potential of the more energetic 98% hydrogen peroxide has been shown to be even better than that of 90% hydrogen peroxide (*2*).

Relatively limited experimental work has been performed with lithium aluminum hydride as a pro-

Northrop Norair, Hawthorne, California.

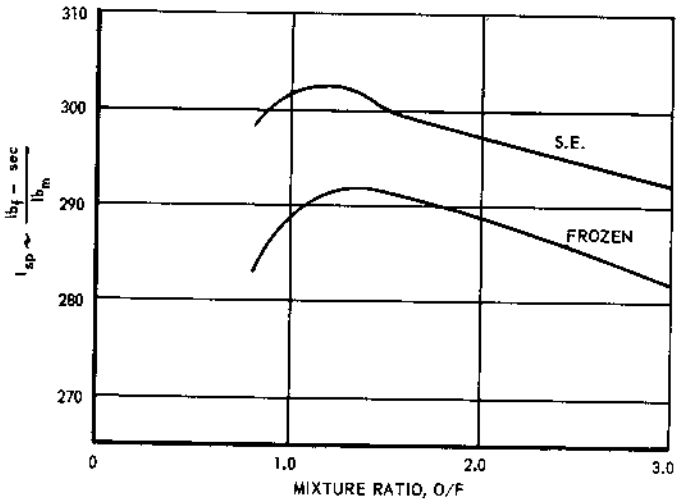

Fig. 1. Specific impulse of 100% hydrogen peroxide–lithium aluminum hydride. Optimum expansion (1,000 ⟶ 14.7 lb./sq. in. abs.).

pellant, although it has been used extensively for the reduction of over sixty different functional groups (*3*). The problem of manufacturing a large scale lithium aluminum hydride fuel grain exists, since lithium aluminum hydride starts to decompose at about 125 °C. and will react with trace amounts of water. Lithium aluminum hydride grain formulation by compression molding is feasible on a small scale as indicated in this paper.

The specific task undertaken here was to establish the combustion characteristics of the propellant combination experimentally. The actual propellants selected for the tests were 90% concentration hydrogen peroxide and 95% lithium aluminum hydride with 5% polyethylene additive. The theoretical performance of this combination is presented in Figure 2 and has a peak *Isp* of 297 sec.

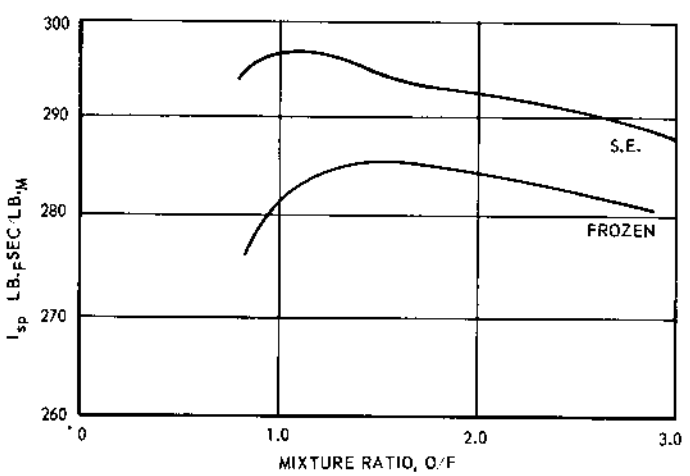

Fig. 2. Specific impulse of 90% hydrogen peroxide–95% lithium aluminum hydride/5% polyethelene. Optimum expansion (1,000 ⟶ 14.7 lb./sq. in. abs.).

APPARATUS AND PROCEDURE

Test firings were conducted at the Propellant Evaluation Facility of the Edwards Air Force Base Rocket Research Laboratory. A scaled drawing of the test hardware is presented in Figure 3 and is shown mounted on the thrust stand in Figure 4.

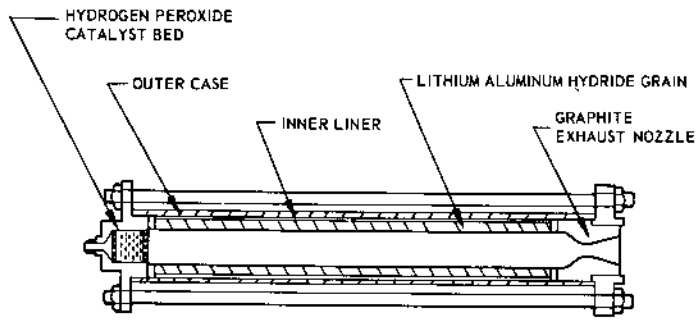

Fig. 3. General configuration of test hardware.

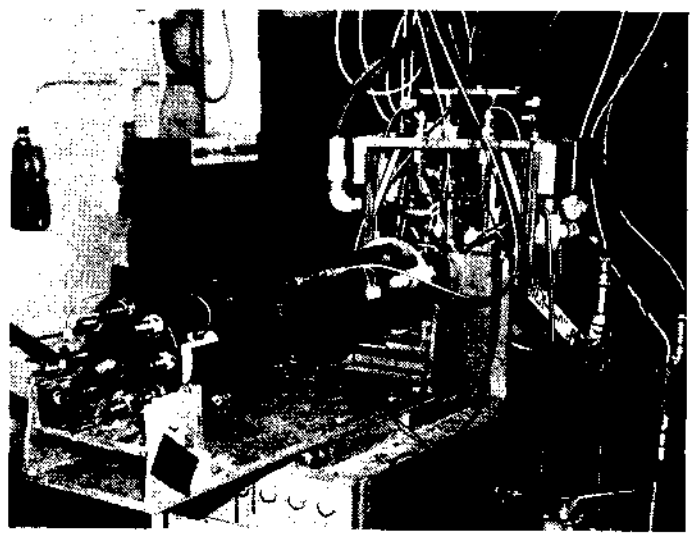

Fig. 4. Test hardward on thrust stand.

Preliminary experiments were performed to determine the percentage of binder that should be added to the solid fuel to enhance its structural properties without unacceptably degrading the theoretical *Isp*. The results of these rather crude, but sufficient tests are summarized in Figure 5. One-half inch diameter lithium aluminum hydride pellets were pressed at formation pressures up to 30,000 lb./sq. in. with no additive, 5 and 10% polyethylene, and with 5% lithium nitride. Pellet lengths varied between ¼ and ⅜ in. The pellets were loaded in the axial direction to the point of crushing with deformation recorded at each load increment. Pellets with 5% Li_3N crushed at a stress about 25% higher than the 100% lithium aluminum hydride pellets at a formation pressure of 30,000 lb./sq. in. At the same formation pressure, the 5% polyethylene pellets had a crushing stress about 17% higher than the 100% lithium aluminum hydride pellets. 10% polyethylene/90% lithium aluminum hydride pellets had the same crushing stress as 100% lithium aluminum

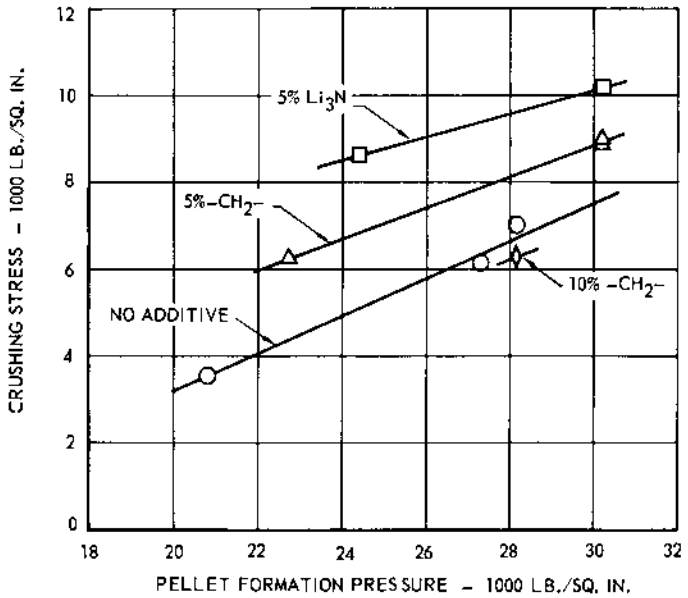

Fig. 5. Summary of pellet stress tests.

hydride. 95% lithium aluminum hydride/5% polyethylene was selected as the combination for the grain formulation because it had a higher theoretical *Isp* (297 sec.) than the 5% lithium nitride combination, and it seemed to have adequate structural properties.

Lithium aluminum hydride was obtained in lump form, ground for ½ to 1 hr. on a ball mill and sifted through a 60-mesh sieve prior to mixing. Polyethylene powder having a particle size equivalent to 50 mesh was added to the batch of powdered lithium aluminum hydride so as to have a mixture of 95% lithium aluminum hydride and 5% polyethylene by weight. This mixture was rolled on a ball mill for up to an hour to ensure a homogeneous mixture. All handling and mixing of the lithium aluminum hydride lump and powder were performed in the dry nitrogen atmosphere of a glove box.

Cylindrical segments of 95% lithium aluminum hydride/5% polyethylene were compression molded at 30,000 lb./sq. in. for test firings and bonded end to end to form a 20 in. long grain having an inside diameter of 1.75 in. and a web thickness of ½ in. A photograph of a finished fuel segment is shown in Figure 6. Segment densities were consistently about 94% of theoretical as shown in Table 1. The fuel grains maintained their structural integrity at all times, even during two firings (no data) which had hard starts due to an accumulation of liquid hydrogen peroxide just prior to ignition.

Ignition of the lithium aluminum hydride grain with the hot decomposed hydrogen peroxide gases was spontaneous.

Thrust, chamber pressure, oxidizer flow rate, tank pressure, and oxidizer feed pressure were recorded during each firing. The hydrogen peroxide temperature was taken prior to each firing. A cavitating Venturi was installed in the hydrogen peroxide feed system and a programmed start was incorporated in the firing procedure after test No. 3. The programmed start introduced a slug of hydrogen peroxide into the decomposition chamber 1 sec. prior to the firing to eliminate the excessive decomposition delay times experienced during previous tests.

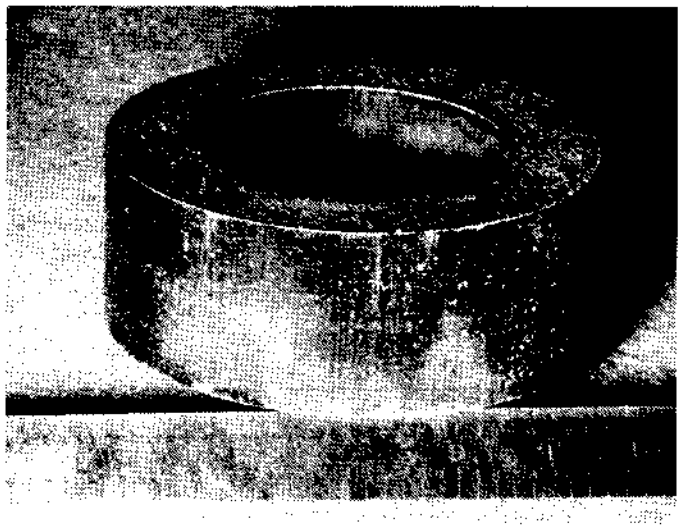

Fig. 6. Grain segment.

TABLE 1. FUEL GRAIN PHYSICAL DATA

	Segments		Grain	
Test No	Average density, ~g./cc.	Percent of theoretical density	Weight, ~g.	Length, ~in.
1	0.877	95.7	1,023.5	20
2	0.862	94.3	1,006.5	20
3	0.865	94.4	1,013.4	20
4	0.868	94.7	1,014.0	20
5	0.864	94.3	903.9	17.82
6	0.862	94.0	897.9	17.75

RESULTS AND DISCUSSION

MEASURED THRUST AND CHAMBER PRESSURE

Average thrust levels ranged from 95 to 220 lb. with chamber pressures of 120 to 404 lb./sq. in. abs., not respectively. Typical data are presented in Figures 7 and 8. A summary of the average data for each test firing is given in Table 2. Oxidizer flow rate was held constant throughout each firing with the exception of test No. 2 which varied slightly owing to tank pressure drift. In all cases, the thrust-time and pressure-time curves were slightly progressive. Fluctuations in the traces are principally the result of a cyclic chamber pressure at the rate of 9 cycles/sec. with amplitudes of about +14 to −7% about the average pressure level. The exact frequency is not discernable from the time traces, as presented in the figures, because the values that went into making up the curves are based on integrating each parameter over a 200 msec. period with points spaced every 100 msec. This was done so that the trend with time could be easily observed. This low frequency of 9 cycles/sec. is not considered to be a combustion instabil-

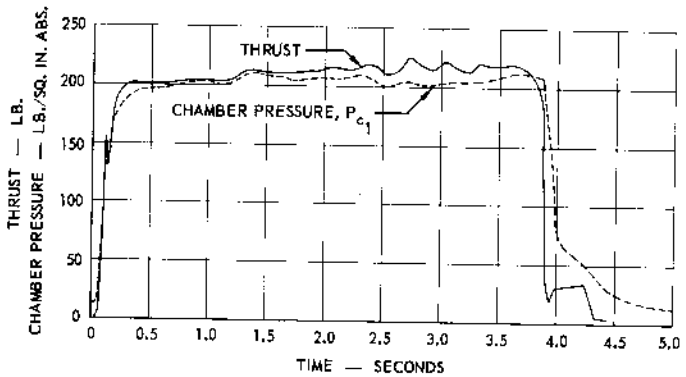

Fig. 7. Thrust and chamber pressure time history for test No. 4.

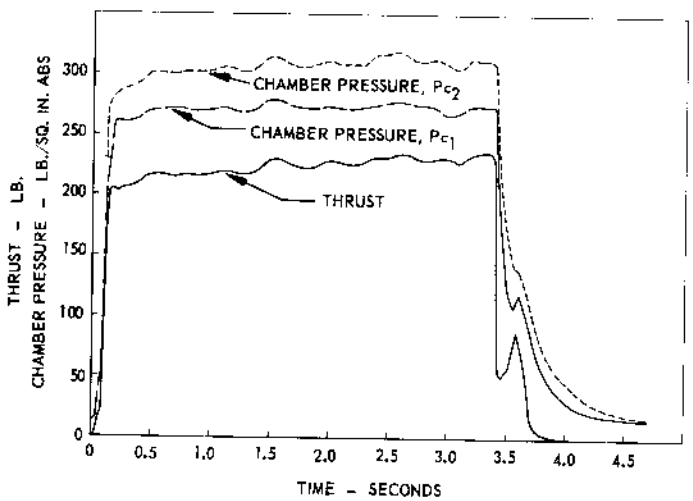

Fig. 8. Thrust and chamber pressure time history for test No. 5. Turbulator in combustion chamber.

ity. The fundamental frequency of the system is on the order of 1,000 cycles/sec.

A possible explanation of the low-frequency phenomenon could be the way the lithium aluminum hydride decomposition products are formed and transported into the boundary layer (see Appendix B for lithium aluminum hydride decomposition products). Since aluminum accounts for 67.5% by weight of the fuel grain, it seems highly possible that a blanket of molten aluminum could be formed over the grain surface which is blown off periodically by the evolution of hydrogen from the parent grain, thus causing periodic reactions leading to the observed low-frequency pressure oscillations. A blanket of molten aluminum has been observed to almost cover the surface of solid propellants containing only 20% aluminum (*4*).

It is felt that the low-frequency phenomenon is not due to the gas generator, since it performed satisfactorily during checkout of the hydrogen peroxide system.

COMBUSTION EFFICIENCY

Some insight may be gained as to the reason for the low combustion efficiencies (indicated by η_{c^*} and η_{Isp}) shown for the test data in Table 2 by examining the following figures:

Melting point of aluminum	1,678 °R.
Calculated flame temperature	4,040 °R.
Boiling point of aluminum	4,200 °R.
Melting point of aluminum oxide	4,172 °R.

The above calculated flame temperature of 4,040 °R. is for test No. 5 and is based on the experimental characteristic velocity. Test No. 5 was selected to make the above comparison because it yielded the highest calculated flame temperature (theoretical flame temperature is about 5,500 °R.). Therefore, if the following argument is valid for test No. 5, it is valid for the other tests.

Liquid aluminum oxide theoretically accounts for 50% by weight of the exhaust products at these test conditions. It is speculated that the size of the particles leaving the surface of the grain is relatively large, much larger than typical aluminum oxide particles (2 to 5 μ) found in combustion products. The deposits left on the exhaust nozzle after each firing, as shown in Figure 9, tend to substantiate this speculation; however, slab tests with provisions for visual observation of the regressing fuel would be needed to prove this. The degree of particle agglomeration that occurs at the surface of the grain is unknown; however, some agglomeration is sure to take place which reduces the available reaction surface. The molten aluminum particles upon leaving the surface will form a protective oxide coating in the oxidizing atmosphere, thereby inhibiting further reaction. If the molten aluminum

TABLE 2. HYBRID DATA SUMMARY

Test No.	Thrust, lb.	Chamber pressure, lb./sq. in. abs.	Mixture ratio	Average regression rate, $\bar{r}$, in./sec.	Measured I_{sp}, sec.	η_{c^*}	η_{Isp}	Remarks
2	95*	120	1.38	0.0691	–	80.6	–	
4	208	207	1.52	0.102	193	84.9	79.7	
5	220	268	1.60	0.111	202	86.0	79.6	Turbulator in combustion chamber
6	131	376	1.59	0.0693	203	78.5	76.7	Turbulator in combustion chamber

*Calculated value.

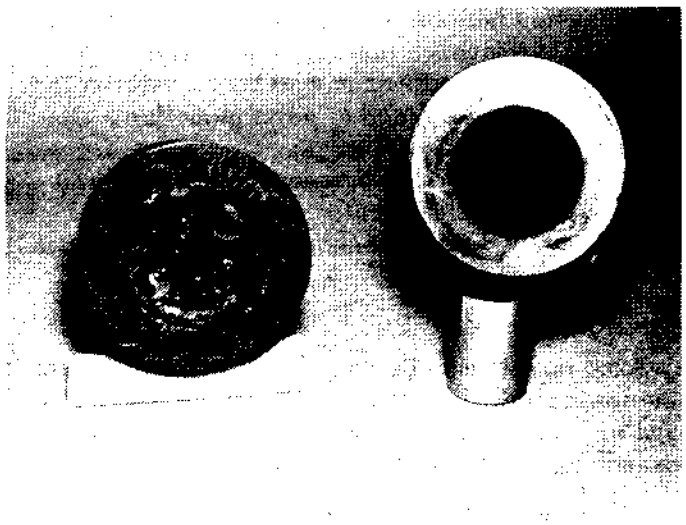

Fig. 9. Turbulator and exhaust nozzle after test firing.

core did not reach its boiling temperature, there would be no driving force to break through the oxide coating, and the particles would leave the combustion chamber intact with an unreacted aluminum core. Aside from the fact that lower efficiencies are predicted (*5*) for small-scale engines having high concentrations of particles in the exhaust products, the most logical explanation of the low C^* efficiencies of 80 to 86% and Isp efficiencies of nearly 80% would then seem to be that relatively large particles leave the surface of the grain and leave the combustion chamber unreacted for the above-mentioned reasons.

A possible method of increasing the combustion efficiency is to substitute powdered aluminum or magnesium for 5 to 10% of the lithium aluminum hydride. Computer studies have shown that the theoretical flame temperature can be increased by about 100° to 150°F./5% aluminum additive at the cost of a slight increase in the amount of condensed phase products. From a practical standpoint, the substitution of aluminum would probably aggravate the particle size agglomeration problem at the grain surface. The effect on flame temperature of adding 10% magnesium is an increase of 100° to 150°F. However, the main expected advantage of magnesium over aluminum arises from the fact that apparently magnesium burns in the vapor phase, while aluminum has a surface reaction (*6*). Since magnesium boils at 2,480°R., it would seem that full advantage could be taken of its heat of combustion as a boot strap to improve the overall combustion efficiency.

TURBULATORS

An effort was made to improve the combustion efficiency through the use of forced mixing devices. A turbulator of the type shown in Figure 9 was located at the downstream end of the fuel grain during test Nos. 5 and 6. The measured total pressure drop through the turbulator ($Pc_2 - Pc_1$) for test No. 5 was about 11%, as can be deduced from Figure 8. The grain was shortened approximately 2 in. to accommodate the graphite turbulator, while the overall combustion chamber length remained the same with essentially no change in volume. There was no significant change in the resulting C^* efficiency of test No. 5 as shown in Table 2. (The actual increase in C^* efficiency of 84.9 to 86.0% is considered to be outside the experimental accuracy.) Test No. 6 actually had a lower efficiency, but the data from this firing are thought to be invalid, as will be explained later.

The fact that the turbulator did not produce a significantly higher combustion efficiency tends to confirm the idea offered in the previous section that the low efficiencies are primarily attributable to the chamber temperature's not being high enough for complete reaction, which in turn is the result of inherently large particles being emitted from the grain, rather than to a lack of sufficient mixing and stay time.

REGRESSION RATE CORRELATION

An attempt was made to correlate the hybrid engine fuel regression rate with an equation that includes both the effects of convective and radiative heat transfer as predicted by theory. The form of this equation from reference 7 is

$$\rho_f \dot{r} = \frac{\dot{Q}_c}{h_v} e^{-\dot{Q}_{rad}/\dot{Q}_c} + \frac{\dot{Q}_{rad}}{h_v}$$

where h_v is the fuel effective heat of gasification. Unfortunately, this approach did not produce a meaningful solution because too many radiation properties are unknown, including the emissivity of the grain wall, emissivity of the gases, optical thickness, and mean particle size. Therefore, the data were correlated in an empirical manner.

A method of determining the length-averaged regression rates $\hat{r}$ was devised based on the assumption of constant characteristic velocity efficiency at any time during the given run. This method is described in detail in Appendix A. The length-averaged regression rates were correlated with oxidizer mass velocity G_{ox} and chamber pressure as shown in Figure 10. G_{ox} is the ratio of oxidizer flow to the average port cross-sectional area at any time. Each curve represents a separate firing and chamber pressure. The slopes of the curves are very nearly equal and have a value of about 0.4. Time progresses from right to left on each curve,

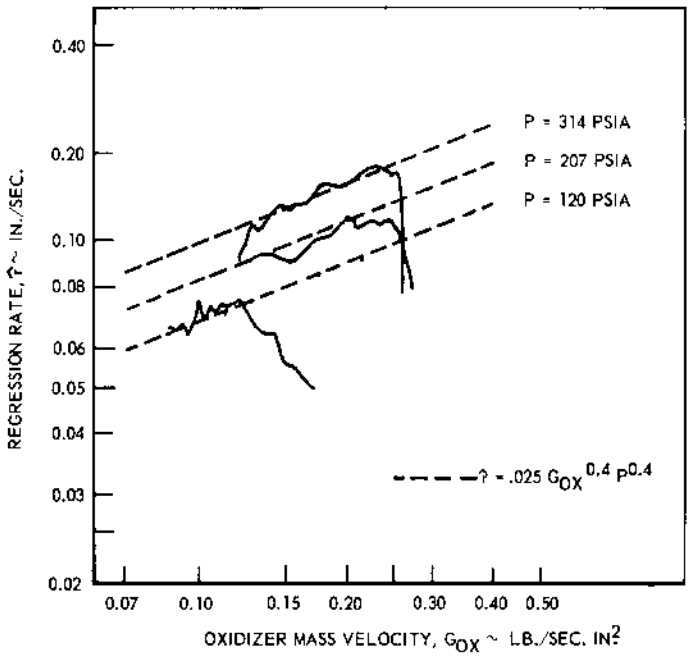

Fig. 10. Fuel regression rate correlation.

increasing as G_{ox} decreases. The initial regression rates are not included in defining the slope because they are considered to be within the transient period during which a steady state temperature profile is being established within the solid fuel grain (7). The regression rate is rising rapidly in this time period and does not lend itself to a steady state treatment. The steady state portion of interest is characterized by an ever decreasing regression rate which is explained by the fact that the heat transfer per unit surface area is always decreasing owing to a relatively constant heat input and increasing surface area. The empirical correlation obtained was

$$\hat{r} = 0.025\, P^{0.4}\, G_{ox}^{0.4} \text{ in./sec.}$$

The regression rate is seen to be moderately pressure sensitive, which is desirable for applications requiring thrust variation. Naturally, many more test firings are required to confirm the indicated pressure sensitivity from a statistical standpoint.

The data from test No. 6 are not presented in Figure 10, nor are they used in obtaining the empirical regression rate equation. It was found that the data from this particular firing could not be correlated with the other three firings, and any correlation including test No. 6 led to the impossible conclusion that regression rate approached zero as chamber pressure increased. Therefore, these data were excluded from the correlation.

A typical time history of the calculated mixture ratios and regression rates is presented in Figure 11. The mixture ratio is seen to decrease very slightly over the test period after the initial start-up transient. A detailed inspection of the regression equation indicates that the mixture ratio will decrease slightly with time for a tubular grain (see Appendix C).

Regression profiles were obtained for two of the firings by making post-run grain port diameter measurements. A typical one is presented in Figure 12. The high regression at the head end is due in part to the expanding decomposed hydrogen peroxide gases. No attempt was made to optimize the injector because a review of the literature indicated that this problem could be solved with some development. The average regression rates based on diameter measurements are slightly lower and within 8% of the average regression rates (given in Table 2) based on weight measurements. Both types of regression rates are based on total run time and total grain length. This apparent discrepancy in regression rates by the two methods is attributed to the char layer (visible in Figure 13) which is less dense than the virgin grain. It can be seen that the surface of the grain is smooth over the aft two-thirds of its length.

GRAIN DESIGN ASPECTS

Certain design aspects of a tubular fuel grain can be deduced for the propellant combination described

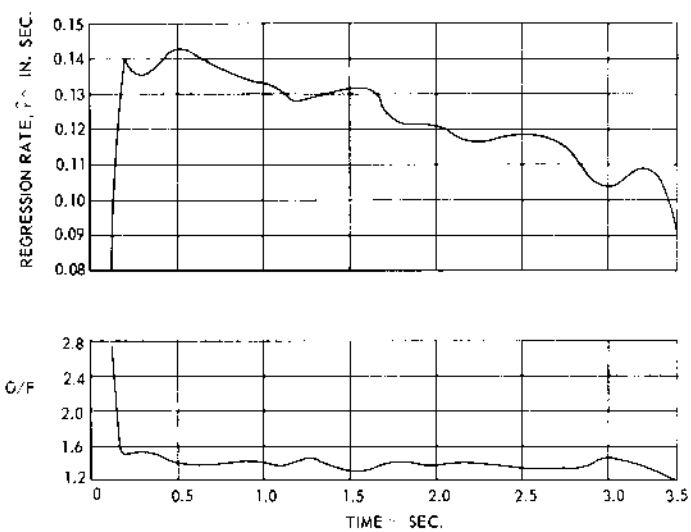

Fig. 11. Calculated $\hat{r}$ and O/F time history for test No. 5.

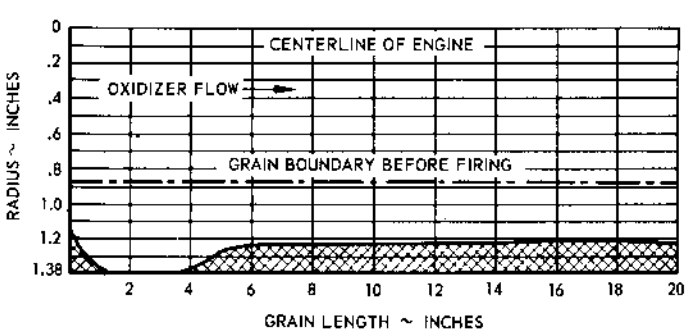

Fig. 12. Post-test fuel regression profile.

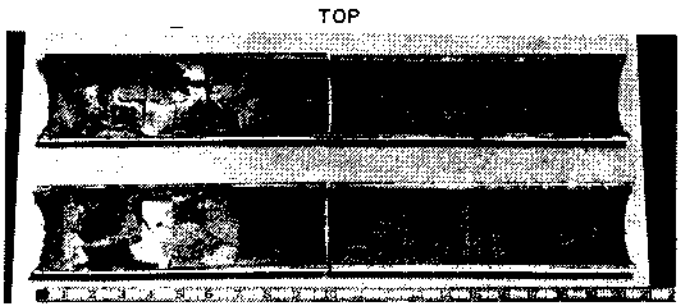

Fig. 13. Partially expended fuel grain.

herein. No implication is intended that scale up effects will not change the regression rate correlation; however, it is of considerable interest to see the relationship between the design parameters based on a pressure sensitive fuel. Therefore, the equations for a tubular grain design are given in Appendix C based on the following conditions:

Initial thrust = 20,000 lb.
Initial P_c = 400 lb./sq. in. abs.
Initial D_p = 12 in.
Initial O/F = 2.0
Grain length = 96 in.
Delivered Isp_{vac} = 319 sec. = constant
Delivered C^* = constant

Other assumptions must be made before the design can be carried through to completion. In particular, a throttling schedule must be assumed, and therein lies the problem resulting from any appreciable shift of mixture ratio with throttling. This is a lengthy task and is beyond the scope of this paper; however, the analysis in Appendix C shows that an oxidizer throttling ratio of 15 : 1 is practical (no aft-end injection), with 25 : 1 being possible during the initial life of the fuel grain. Hybrid engine studies (*8*) indicate that an oxidizer throttling ratio of 25 : 1 corresponds to a thrust variation of about 18 : 1, and an oxidizer throttling ratio of 15 : 1 corresponds to a thrust variation of 11 : 1. Associated with the 15 : 1 oxidizer throttling is a reduction of O/F by a factor 1.9 during the initial life of the grain.

By the way of contrast, a nonpressure sensitive hybrid fuel that obeys the typical regression law of the type

$$\hat{r} = a\, G_{ox}^{\,b}$$

where $b = 0.4$, can only be throttled by 4 : 1 for the same change in O/F. Therefore, it can be seen that pressure sensitivity considerably improves the hybrid rocket engine throttling capability.

CONCLUSIONS

The combustion and performance characteristics of lithium aluminum hydride were investigated experimentally with 90% hydrogen peroxide as the oxidizer. The test results and subsequent analyses indicate the following conclusions.

1. The length average fuel regression rate, based on limited data, is pressure sensitive and obeys the empirical equation

$$\hat{r} = 0.025\, P^{0.4}\, G_{ox}^{0.4}$$

2. Based on this regression correlation, it is practical to vary the thrust of a hybrid engine by using these propellants with a O/F variation which can be small. A typical design case gave only a 2 : 1 reduction in O/F for 11 : 1 thrust reduction.

3. Experimental values of Isp and C^* efficiencies were 80 and 80 to 86%, respectively, for a small-scale engine with gaseous oxidizer injection.

4. Forced mixing at the aft end of the tubular grain did not significantly increase the combustion efficiency.

5. The combustion inefficiency is primarily attributed to the incomplete reaction of the aluminum particles due to the low chamber temperature.

6. The strength properties of the pressed grains were adequate, since structural problems were not encountered during the firings.

7. The grain surface was smooth over the 70% of its length that had not regressed to the liner.

ACKNOWLEDGMENT

Grateful acknowledgment is made to the following people who contributed to the accomplishment of the research program described here. Research: G. R. Hall, Aaron Feder, J. A. Bogdanovic, and Rahim Lavi. Test operations: J. H. Rudy, M. A. Mather, and R. F. Basch.

NOTATION

A_t = nozzle throat area, sq. in.
A^* = average of prefiring and postfiring nozzle throat areas, sq. in.
C^* = characteristic velocity, ft./sec.
D_o = grain port diameter at time zero, in.
D_p = grain port diameter (average with respect to length) at any time, in.
F = thrust, lb.
g = acceleration due to gravity, 32.174 ft./sec.^{2}
G_{ox} = oxidizer mass velocity, $\dot{W}_{ox}/\frac{\pi}{4} D_p^2$, lb./(sq. in.)(sec.)
Isp = specific impulse, $(lb._f)(sec.)/lb._m$
L = grain length, in.
O/F = mixture ratio, $\dot{W}_{ox}/\dot{W}_f$
P or P_c = chamber pressure, lb./sq. in. abs.

R_o = radius of cylindrical grain at time zero, in.
R_p = average radius of grain at any time, in.
$\dot{r}$ = regression rate, in./sec.
$\hat{r}$ = regression rate averaged over the grain length at any time, in./sec.
$\overline{r}$ = average (with respect to time and length) regression rate, in./sec.
R_{tot} = total regression, in.
t = time, sec.
$\dot{W}_f$ = fuel flow rate, lb./sec.
$\dot{W}_{ox}$ = oxidizer flow rate, lb./sec.
$\dot{W}_t$ = total propellant flow rate, lb./sec.

GREEK LETTERS

ε = nozzle expansion ratio
η_{c^*} = characteristic velocity efficiency
η_{Isp} = specific impulse efficiency
ρ_f = fuel grain density, lb./cu. in.
ΔW_f = weight of fuel regressed, lb.

SUBSCRIPTS

B = burn or reference
i = initial (with respect to time)
meas. = measured

LITERATURE CITED

1. Brown, H. N., and Mary M. Williams, U. S. Naval Ordnance Test Station, China Lake, Calif., *NAVWEPS Rept.* 7043 (June, 1960).
2. McCormick, J. C., "Excellent Storage Record with Becco 90% and 98% H_2O_2," FMC Corp. (1963).
3. Hinckley, A. A., Metal Hydrides Inc., *Bull. No. 401* (October, 1963).
4. Watermeier, L. A., W. P. Aungst, and S. P. Pfaff, "Experimental Study of the Aluminum Additive Role in Unstable Combustion of Solid Rocket Propellants," p. 316, Ninth Symposium (International) on Combustion, Academic Press, New York (1963).
5. Hall, G. R., Northrop Corp. Norair Div., *NOR 63-42* (March, 1963).
6. Gordon, D. A., in "Solid Propellant Rocket Research," M. Summerfield, ed., p. 271, Academic Press, New York (1960).
7. Marxman, G. A., C. E. Wooldridge, and R. J. Muzzy, United Technology Center, Sunnyvale, Calif. *AIAA Preprint No. 63-505* (December, 1963).
8. Bogdanovic, J. A., private communication to the author.
9. JANAF Thermochemical Tables (June, 1963).

APPENDIX A

GENERAL METHOD OF DATA REDUCTION

The test firings were treated as a single impulse for purposes of calculating average values of C^* and Isp efficiencies. The reference run time was defined as the oxidizer flow time (the time from the first to the last movement in the oxidizer cycle per second trace on the oscillogram). Reference run times varied between 3.4 and 3.9 sec. Average thrust and chamber pressure is based on integrating all the area under the curve as shown in Figure A1 and dividing by the length corresponding to the reference run time. Therefore, the average values of the performance parameters were calculated:

$$\overline{C^*} = \frac{gA^* \int_0^{\infty} P_c \, dt}{\Delta W_f + \int_0^{t} \dot{W}_{ox} \, dt} \tag{A1}$$

$$\overline{Isp} = \frac{\int_0^{\infty} F \, dt}{\Delta W_f + \int_0^{t} \dot{W}_{ox} \, dt} \tag{A2}$$

$$\overline{O/F} = \int_0^{t} \dot{W}_{ox} \, dt / \Delta W_f \tag{A3}$$

Note that none of the above expressions involve specification of an ambiguous time.

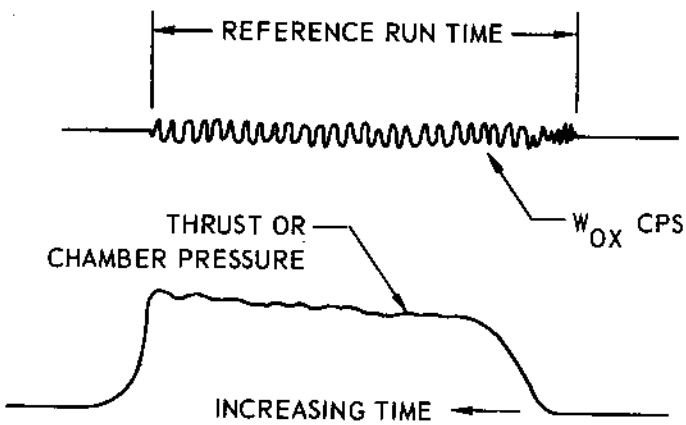

Fig. A1. Sketch showing reference run time.

REGRESSION RATE MEASUREMENTS

The average regression rate $\overline{r}$ is based on fuel grain weight measurements made before and after each firing and therefore takes into account the fore end grain irregularity. These values are listed in Table 2. The procedure for calculating the average regression rate is given below. It is assumed that the surface of the fuel grain regresses cylindrically; therefore, the measured weight of fuel regressed is

$$\Delta W_f = \rho_f (\Delta \text{ Vol.}) = \rho_f \pi L (R_p^2 - R_o^2)$$

Therefore

$$R_p^2 - R_o^2 = \frac{\Delta W_f}{\rho_f \pi L}$$

and

$$R_p = \left(\frac{\Delta W_f}{\rho_f \pi L} + R_o^2 \right)^{1/2}$$

By definition, the average regression rate $\overline{r}$ is

$$\overline{r} = \frac{R_p - R_o}{t_B}$$

Substitution for R_p yields $\bar{r}$ in terms of known quantities:

$$\bar{r} = \frac{1}{t_B}\left[\left(\frac{\Delta W_f}{\rho_f \pi L} + R_o^2\right)^{1/2} - R_o\right] \quad \text{(A4)}$$

CONSTANT C* EFFICIENCY ANALYSIS

The assumption was made that the characteristic velocity efficiency is constant throughout the firing and that its value is equal to that calculated from the average characteristic velocity, $\bar{C}^*$. This assumption permits the calculation of instantaneous† values of regression rate, mixture ratio, and oxidizer mass velocity. Therefore, at any time t

$$\eta_{c^*} C^* = C^*_{\text{meas.}} = \frac{P_c A^* g}{\dot{W}_{ox} + \dot{W}_f}$$

Fuel flow rate may be written in two ways:

$$\dot{W}_f = \frac{P_c A^* g}{\eta_{c^*} C^*} - \dot{W}_{ox}$$

$$\dot{W}_f = \rho_f (\pi D_p L)\hat{r}$$

and

$$D_p = D_o + 2\int_0^t \hat{r}\, dt$$

Equating the two $\dot{W}_f$ equations and solving for $\hat{r}$ one gets

$$\hat{r} = \frac{1}{\rho_f (\pi D_p L)}\left[\frac{P_c A^* g}{\eta_{c^*} C^*} - \dot{W}_{ox}\right] \quad \text{(A5)}$$

The mixture ratio at any time is given by

$$O/F = \frac{\dot{W}_{ox}}{\rho_f (\pi D_p L)\hat{r}}$$

or

$$\hat{r} = \frac{\dot{W}_{ox}}{(O/F)\rho_f (\pi D_p L)} \quad \text{(A6)}$$

Equating Equation (A5) and (A6) and rearranging, one obtains the final expression for mixture ratio:

$$O/F = \frac{1}{\dfrac{P_c A^* g}{\dot{W}_{ox}\eta_{c^*} C^*} - 1} \quad \text{(A7)}$$

The calculation of O/F at any time t from Equation (A7) requires an iterative procedure, since C^* is a function of O/F. Usually, one or two iterations are adequate to produce a final O/F within 0.2% of the previous O/F which, of course, is considerably within the accuracy of the method.

To facilitate the calculation of $\hat{r}$ from Equation (A5), the following simplification is made.

Let $$D_p \simeq D_o + 2R_{\text{tot}} + 2\Delta t \hat{r}_{t-\Delta t}$$

where R_{tot} = summation of the incremental regressions for all previous points of calculation
$\hat{r}_{t-\Delta t}$ = calculated regression rate at the previous point

†Instantaneous is taken here to mean a value averaged over a 200-msec. period. The chamber pressure values used in this analysis are based on integrating the raw data over a 200-msec. period every 100 msec.

Therefore $$\hat{r}_1 = \frac{\dot{W}_{ox}\left[\dfrac{P_c A^* g}{\dot{W}_{ox}\eta_{c^*} C^*} - 1\right]}{\rho_f \pi L (D_o + R_{\text{tot}} + 2\Delta t \hat{r}_{t-\Delta t})} \quad \text{(A8)}$$

Again, an iterative procedure is required to reduce the error in $\hat{r}$ resulting from the linearized approximation of D_p. Iteration of $\hat{r}$ is performed by adjusting $\hat{r}_1$ in the following manner;

$$\hat{r}_n = \hat{r}_1 \frac{(D_o + 2R_{\text{tot}} + 2\Delta t \hat{r}_{t-\Delta t})}{(D_o + 2R_{\text{tot}} + 2\Delta t \hat{r}_{n-1})}$$

Two iterations are sufficient to obtain good accuracy. When one knows the instantaneous D_p from the final iteration, then the oxidizer mass velocity is calculated:

$$G_{ox} = \frac{\dot{W}_{ox}}{\left(\dfrac{\pi}{4} D_p^2\right)} \quad \text{(A9)}$$

The effect on these calculated data of an arbitrary change in η_{c^*} at any time during a run has been estimated. A 1% change in η_{c^*} produces a corresponding 2.3% change in O/F, an inverse 2.1% change in $\hat{r}$, and negligible change in mass velocity.

APPENDIX B

PROPERTIES OF LITHIUM ALUMINUM HYDRIDE

Lithium aluminum hydride is a nonvolatile, white crystalline solid. It may turn gray upon standing with no apparent loss in purity or strength. The known physical properties of lithium aluminum hydride are very limited. The currently established data from reference *3* are given below:

Density	0.917 g./cc.
Specific heat	0.48 $\frac{\text{cal.}}{\text{g.-}^\circ\text{K.}}$
ΔH_f	− 24.08 $\frac{\text{kcal.}}{\text{mole}}$

Reference *9* establishes the heat of formation at − 26.2 $\frac{\text{kcal.}}{\text{mole}}$.

Thermal decomposition of lithium aluminum hydride starts without melting at 125° to 135°C. in dry air. The reaction takes place in two stages (*3*), the first of which is the following:

$$LiAlH_4 \longrightarrow LiAlH_2 + H_2$$

This is followed by a slower reaction yielding lithium hydride, aluminum, and more hydrogen:

$$LiAlH_2 \longrightarrow LiH + Al + 1/2\ H_2$$

Solid lithium aluminum hydride is stable at room temperature if not exposed to moisture. Exposure of the solid hydride to moist air causes a relatively slow decomposition, and a protective coating of lithium aluminate forms over the hydride. Pressed segments of $LiAlH_4$ in the presence of excess water will ignite and burn slowly.

APPENDIX C

GRAIN DESIGN EQUATIONS

In order to determine the effect of throttling on mixture ratio change for a tubular fuel grain, a typical calculation is given below for vacuum operation. The following assumptions are made:

1. Oxidizer	90% H_2O_2
2. Fuel	95% $LiAlH_4$/ 5%-CH_2-
3. Regression rate obeys the law	$\hat{r} = 0.025\, P^{0.4}\, G_{ox}^{0.4}$
4. Delivered vacuum $Isp \simeq$ constant	= 319 sec.
5. Initial chamber pressure	= 400 lb./sq. in. abs.
6. Initial thrust	= 20,000 lb.
7. Nozzle expansion ratio	= 50 : 1
8. Grain density	= 0.0313 lb./cu. in.

If the mission requires a constant thrust for any given time increment, then the oxidizer flow must be continually decreased at a rate that will balance the increase in chamber pressure. For simplicity, it will be assumed here that $\dot{W}_{ox}$ will be constant for any nominal thrust level and that the slightly progressive thrust will be acceptable to the mission.

Initial total propellant flow rate

$$(\dot{W}_t)_i = \frac{F}{Isp} = \frac{20{,}000}{319} = 62.8 \text{ lb./sec.}$$

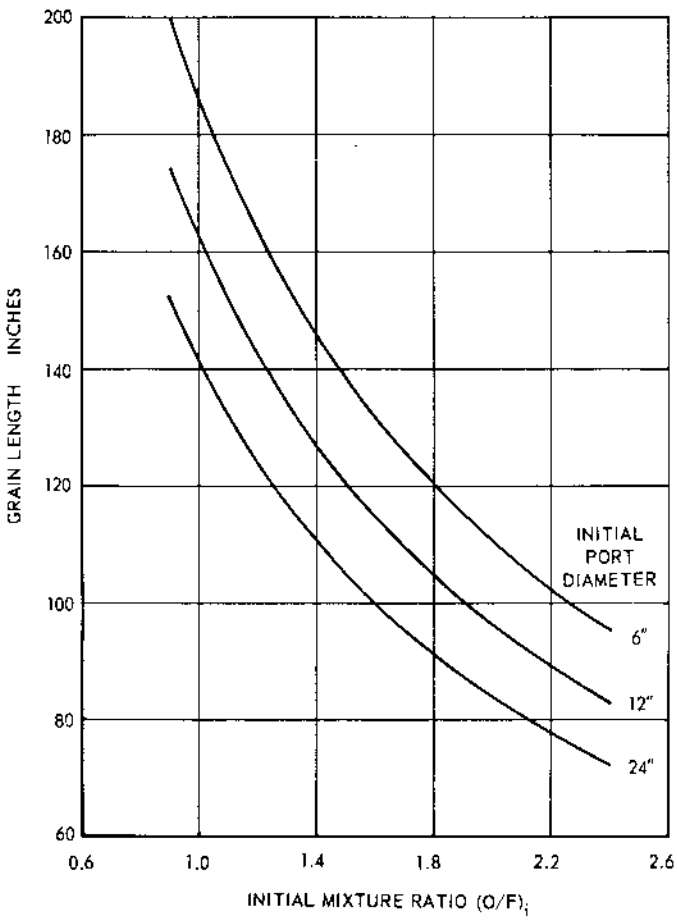

Fig. C1. Tubular grain design. Length vs. initial O/F.

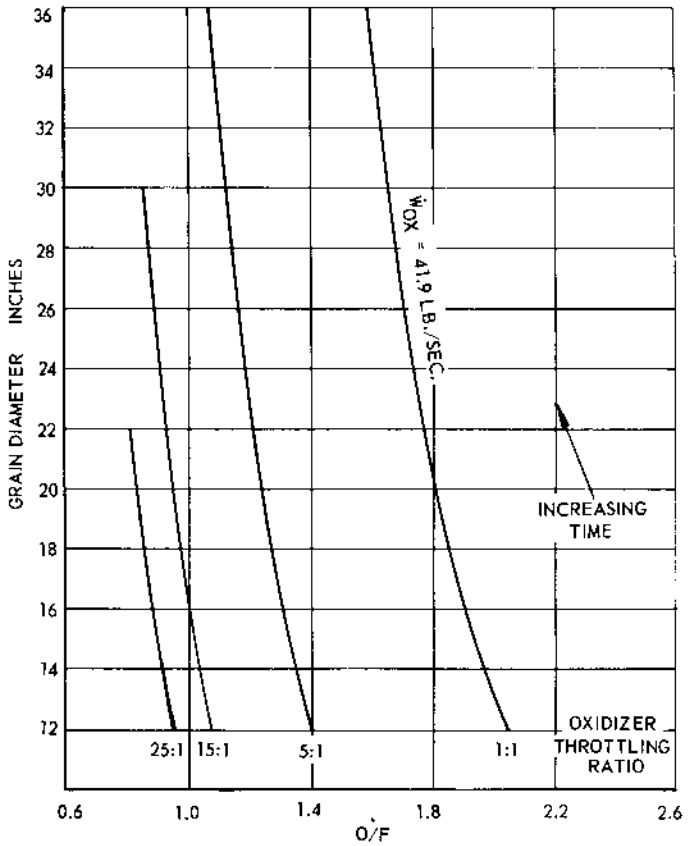

Fig. C2. Grain diameter vs. O/F for various oxidizer throttling ratios. Initial conditions: Dp = 12 in., O/F = 2.0, P_c = 400 lb./sq. in. abs., thrust = 20,000 lb.

Oxidizer flow rate

$$\dot{W}_{ox} = \frac{(O/F)_i}{(O/F+1)_i}\, 62.8$$

Fuel flow rate

$$\dot{W}_f = \hat{r}\,\pi\, D_p\, L\, \rho_f$$

$$= 0.025\, P^{0.4} \left[\frac{\dot{W}_{ox}}{\frac{\pi}{4} D_p^{\,2}}\right]^{0.4} \pi\, D_p\, L\, \rho_f$$

$$\dot{W}_f = 0.002708\, P^{0.4}\, \dot{W}_{ox}^{0.4}\, D_p^{0.2}\, L \qquad \text{(C1)}$$

Grain length

$$O/F = \frac{\dot{W}_{ox}}{0.002708\, P^{0.4}\, W_{ox}^{0.4}\, D_p^{0.2}\, L}$$

$$L = \frac{369.2\, \dot{W}_{ox}^{0.6}}{P^{0.4}\, D_p^{0.2}\, (O/F)_i} \qquad \text{(C2)}$$

$$L = \frac{4{,}431}{P^{0.4}\, D_p^{0.2}\, (O/F+1)_i^{0.6}\, (O/F)_i^{0.4}} \qquad \text{(C3)}$$

This relationship is presented in Figure C1 for initial diameters of 6, 12, and 24 in. Let the initial O/F = 2.0 and the initial grain inside diameter = 12 in. This fixes the grain length at 96 in. and $\dot{W}_{ox}$ at 41.9 lb./sec. Now a relationship between O/F and D_p at any time can be

obtained based on the assumption that the delivered C^* is approximately constant. This assumption is not quite true, especially when the engine is throttled; however, the error should be small.

Nozzle throat area

The vacuum thrust coefficient $\simeq 1.90$ for $\varepsilon = 50$

$$A_t = \frac{20{,}000}{1.90(400)} = 26.3 \text{ sq. in.}$$

Mixture ratio

$$P = \frac{\eta_{c^*} C^* \dot{W}_{ox} (O/F + 1)}{A_t g (O/F)}$$

$$= \frac{5{,}273 \dot{W}_{ox} (O/F + 1)}{26.3(32.174)(O/F)}$$

$$P = 6{,}231 \dot{W}_{ox} \frac{(O/F + 1)}{O/F} \qquad \text{(C4)}$$

Substitution of Equation (C4) into (C2) yields

$$O/F = \frac{369.2 \dot{W}_{ox}^{0.6} (O/F)^{0.4}}{2.08 \dot{W}_{ox}^{0.4} (O/F + 1)^{0.4} D_p^{0.2} 96}$$

$$(O/F)^{0.6} (O/F + 1)^{0.4} = 1.867 \left(\frac{\dot{W}_{ox}}{D_p} \right)^{0.2} \qquad \text{(C5)}$$

The relationship of O/F and D_p in Equation (C5) is presented in Figure C2 for four constant oxidizer flow rates which correspond to oxidizer throttling ratios of 1 : 1, 5 : 1, 15 : 1, and 25 : 1. It appears that a throttling ratio of 15 : 1 is practical and 25 : 1 is possible at early times in the grain life. There is no closed form for determining the thrust and chamber pressure variation with time that corresponds to any point on Figure C2. A point-by-point analysis is required with sufficiently small time increments. This procedure is probably best handled by a computer program; however, the equations are straightforward, as indicated above.